

## X-33 XRS-2200 Linear Aerospike Engine Sea Level Plume Radiation

M. G. D'Agostino, Y. C. Lee, T. S. Wang  
NASA Marshall Space Flight Center, Huntsville Alabama

### ABSTRACT

Wide band plume radiation data were collected during 10 sea level tests of a single XRS-2200 engine at the NASA Stennis Space Center in 1999 and 2000. The XRS-2200 is a liquid hydrogen / liquid oxygen fueled, gas generator cycle linear aerospike engine which develops 204,420 lbf thrust at sea level. Instrumentation consisted of six hemispherical radiometers and one narrow view radiometer. Test conditions varied from 100% to 57% power level (PL) and 6.0 to 4.5 oxidizer to fuel (O/F) ratio. Measured radiation rates generally increased with engine chamber pressure and mixture ratio. 100% power level radiation data were compared to predictions made with the FDNS and GASRAD codes. Predicted levels ranged from 42% over to 7% under average test values.

### INTRODUCTION

The XRS-2200 engine was intended for use on the X-33 lifting body sub-orbital single stage to orbit demonstrator vehicle. XRS-2200 specifications are listed in table I.

Table I, XRS-2200 Engine Specifications

Type:	Linear Aerospike Gas Generator Cycle
Thrusters:	Circular throat / rectangular exit, 5.8:1 area ratio, 10 per side
Propellants:	Liquid Oxygen, Liquid Hydrogen
Thrust:	
At Sea Level:	204,420 lbf
In Vacuum:	266,230 lbf
Specific Impulse:	
At Sea Level:	339.0 sec
In Vacuum:	436.5 sec
Chamber Pressure:	857 psia @ 100% PL
Throttling:	50-100%
Differential Throttling:	±15%
Max. Mixture Ratio (O/F):	6.0
Overall Area Ratio:	57.7:1
Dimensions:	
Forward End:	134 in. wide X 90 in. long
Aft End:	42 in. wide X 90 in. long
Forward to Aft :	90 in.

The unconventional X-33 / XRS-2200 caused uncertainty in plume radiation environment predictions. For this reason, MSFC initiated a test program to measure plume radiation during engine ground tests to increase confidence in our flight environments. This paper presents a summary of the results from wide band infrared plume radiation measurements and analytical predictions. A more complete data set can be found in reference 1.

## TEST SETUP

In the final configuration, six primary instruments were used to measure plume heat flux. Five of the six instruments were 180° hemispherical field of view (FOV) wide angle radiometers. One 4° FOV radiometer was also used.

Table II, Instrument Locations

ID	DESCRIPTION	FOV (°)	LOCATION (INCHES)			POINTING TOWARDS (INCHES)		
			X	Y	Z	X	Y	Z
R101	EECO INNER AFT	180	-38.625	-133.375	-21.500	+	-133.375	-21.500
R101B	EECO INNER AFT MIRRORED	180	-38.625	45.375	-21.500	+		-21.500
R105	NEAR THRUSTER 22°	180	-44.625	-53.750	48.625	N/A	N/A	N/A
R201	THRUSTER SIDE INNER AFT	180	-53.000	-38.375	79.750	+	-38.375	79.750
R202	THRUSTER SIDE OUTER INBOARD	180	-54.750	-43.500	116.750	-54.750	-43.500	-
R203	THRUSTER SIDE OUTER AFT	180	-53.000	-40.250	118.250	+	-40.250	118.250
R207	BELOW THRUSTER INBOARD	180	21.000	-44.750	-151.500	21.000	-44.750	+
R210	BELOW THRUSTER INBOARD NARROW	4	20.000	-44.750	-151.500	20.000	-44.750	+

Instrument locations are shown in table II. R101 and R101B were used for diagnostic purposes. The six primary locations were selected to ensure comprehensive coverage of several plume views and to provide similar orientations to flight test instruments. Radiometer R105 was in close proximity to the engine near the cowl and thruster area on the ramp side to the southeast of the engine as shown in figures 1 through 3. It was mounted directly to the engine/stand interface hardware. The other five were located to the side perpendicular to the engine long axis.

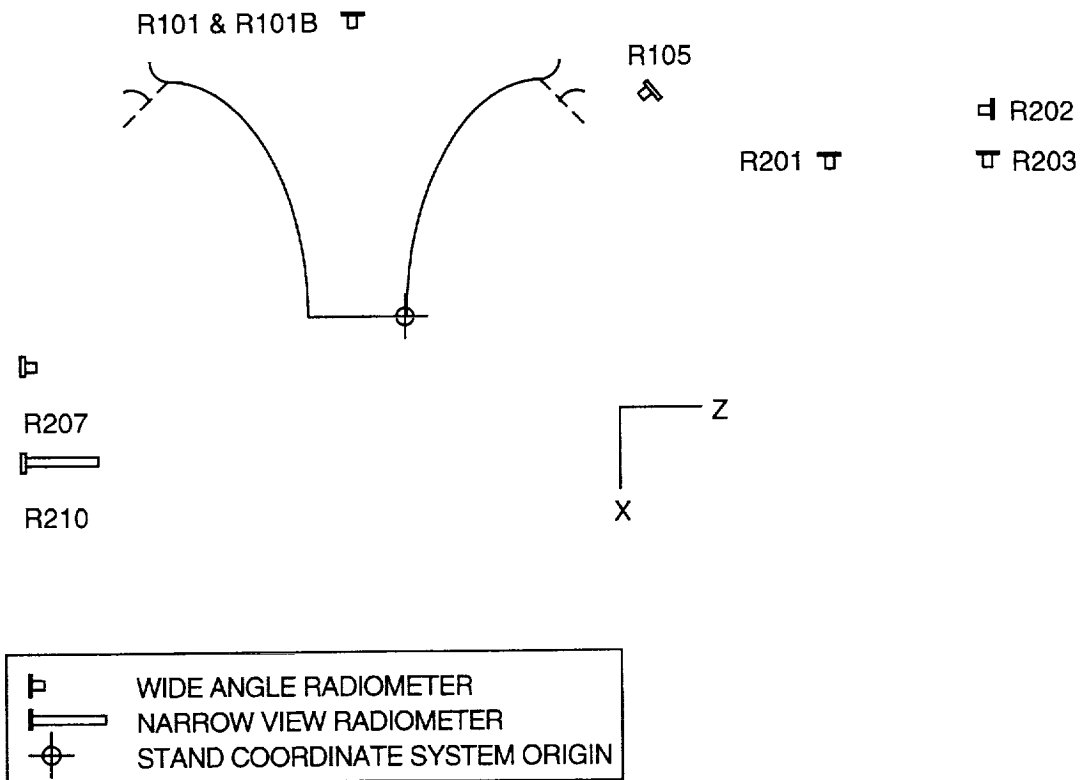


Figure 1, Instrumentation EECO View

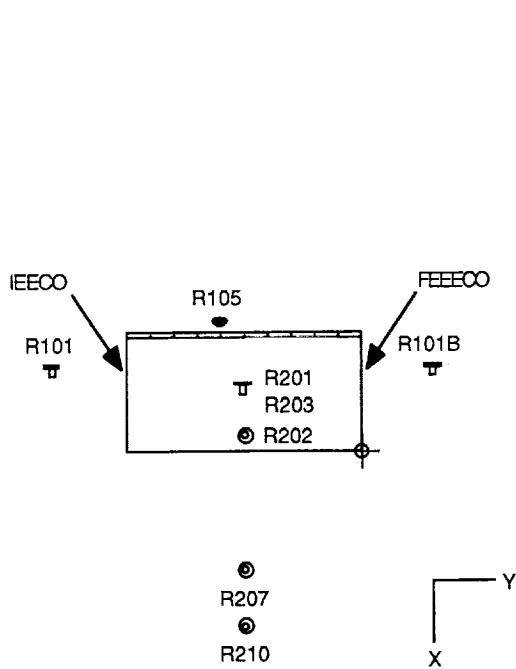


Figure 2, Instrumentation Side View

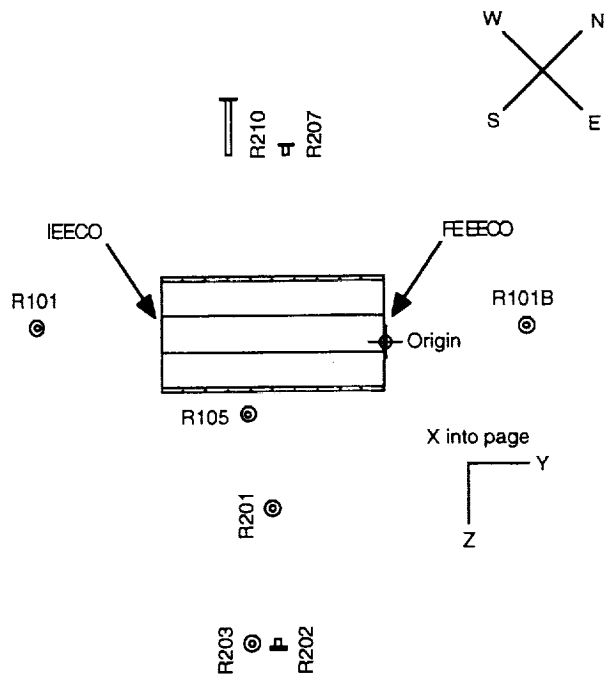


Figure 3, Instrumentation Above View

## RESULTS

The X-33 was to use two XRS-2200 engines joined together at the Inter-Engine End Close-Outs (IEECO). Therefore, the IEECO did not need thermal protection in its flight dual engine configuration. However, during single engine tests, the IEECO had to be thermally protected with a set of cooling water tubes installed on the IEECO end of each ramp.

The base area radiometers were originally located on the IEECO side of the engine. After data from tests 21 and 22 were examined, it became apparent that the IEECO cooling water was attenuating plume radiation to the instruments mounted on that side of the engine. To investigate this, location R101B was installed in a mirror image location to R101 in the +Y direction during test 23 as shown in figures 1 through 3. Figure 4 shows how the data from the two mirrored locations substantially differed. The R101B instrument read over 2 times higher than R101, and was also very close to the predicted level. After test 23, it was decided to move all IEECO instruments to the Flight End Engine End Close-Out (FEEECO) side. This move was never made because at the same time, cooling water was added to the FEEECO.

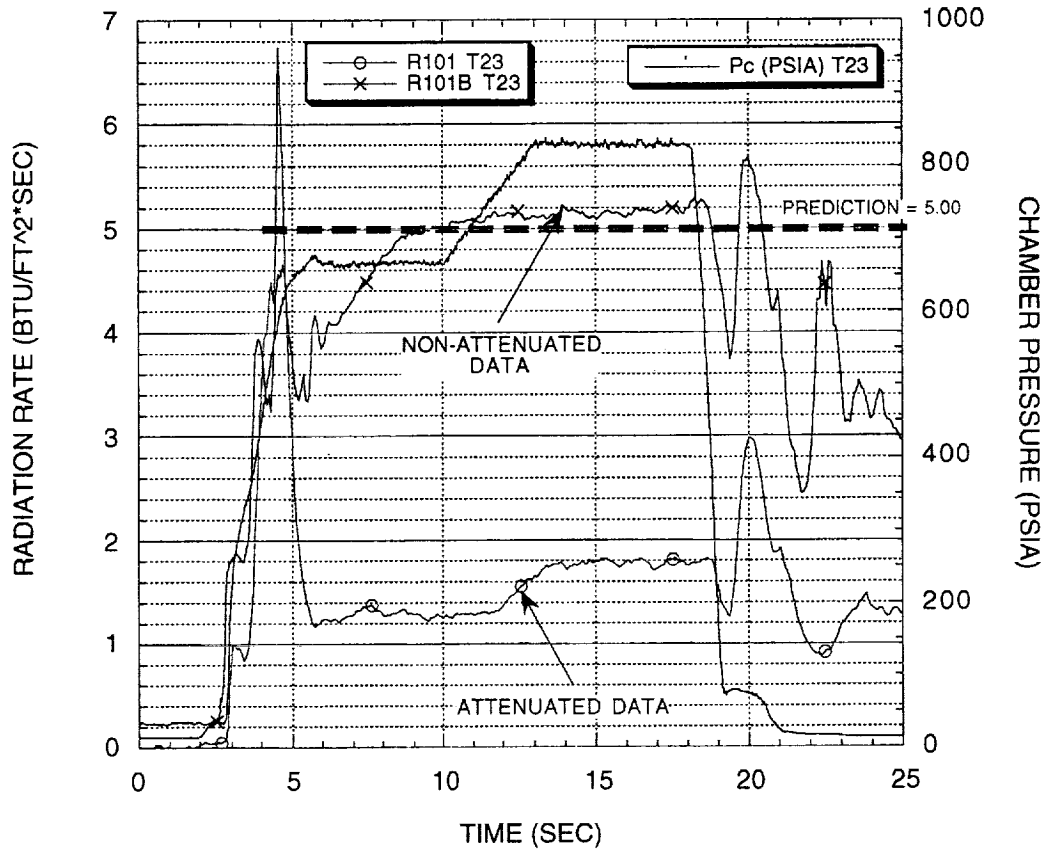


Figure 4, Data From Mirrored Locations R101 and R101B

The FEEECO also requires thermal protection at all times. Damage to the FEEECO was observed in the early tests such that starting with test 24, an ablative material was added to the FEEECO with cooling water flowing behind the ablator. Figure 5 shows a typical view of an engine firing with cooling water. The cooling water from both EECO's is clearly evident.

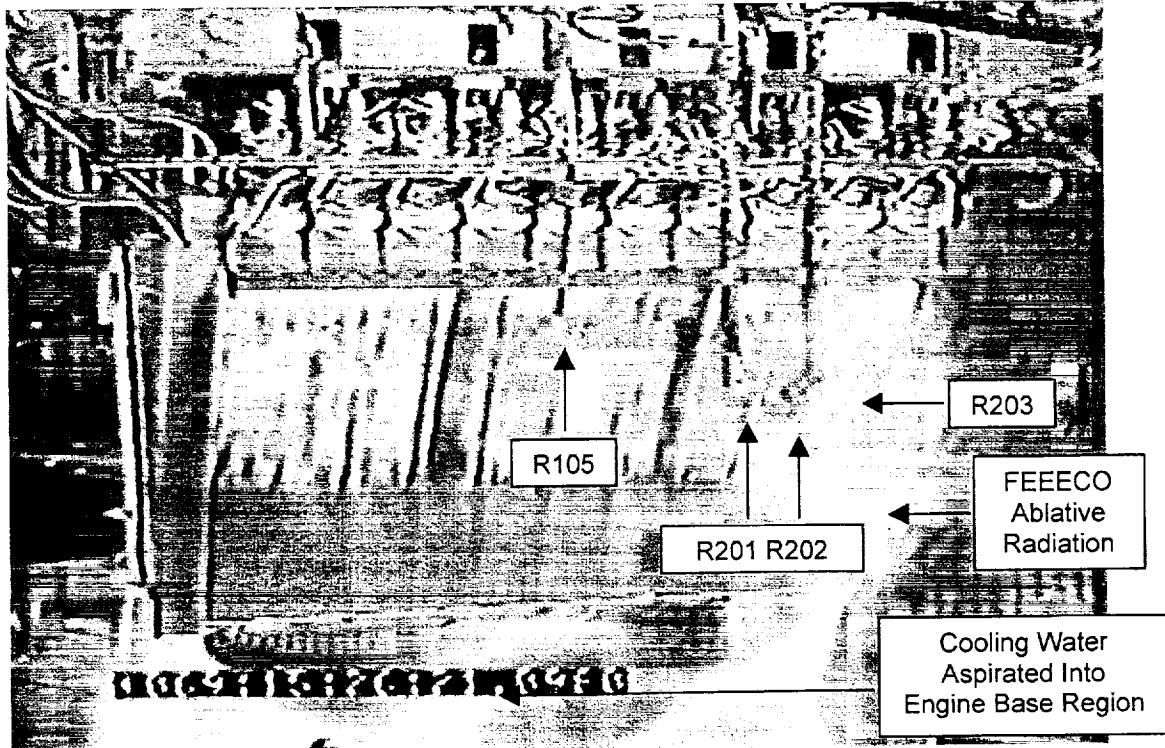


Figure 5, Engine test with cooling water from both EECO's. IEECO on left.

To avoid water cooling effects from both EECO's as much as possible, the five affected locations were moved to positions perpendicular to the engine ramp, 90° away from their original positions. This was done starting with test 27 and the instrument numbers were changed to R201, R202, R203, R207, and R210. The data from these new locations proved to be largely unaffected by the EECO cooling water. All data from tests prior to test 27 was therefore ignored except for R105.

## DATA

Data were collected for a wide variety of test conditions. Test data from O/F and PL settings that were repeated at least once and are tabulated in Table III. Table III consists only of data taken during constant O/F and PL conditions.

Table III, Primary Instrument Test Data

All data in (BTU/ft <sup>2</sup> *sec)	PL (%):	57	63	70	80	98	100	100
	Average Pc (psia):	478	525	583	672	818	838	833
	MR (O/F):	4.5	5.0	5.4	5.5	5.7	5.5	6.0
NEAR THRUSTER 22°	R105	8.9	7.8	8.5	11.1	9.6	10.7	10.7
THRUSTER SIDE INNER AFT	R201	4.6	3.9	4.2	5.3	4.5	5.2	5.7
THRUSTER SIDE OUTER INBOARD	R202	4.4	4.9	5.1	5.3	5.9	5.8	6.2
THRUSTER SIDE OUTER AFT	R203	3.5	2.9	3.2	3.7	3.6	3.8	4.3
BELOW THRUSTER INBOARD	R207	7.7	8.7	8.9	7.7	10.4	9.6	10.8
BELOW THRUSTER INBOARD NARROW	R210	10.3	13.2	12.2	8.8	12.7	13.2	14.4

Data trends from the primary wide angle radiometers (R201 through R207) are generally consistent. Figures 6 through 9 show trends with varying PL at constant O/F. Data is normalized by 80% PL measurements except for Figure 9, which is normalized by 74% measurements because 80% PL was

not run at O/F = 6.0. Wide angle radiometer data generally increases with chamber pressure ( $P_c$ ) and in turn PL. This makes intuitive sense since plume size should increase with  $P_c$  and chamber temperature ( $T_c$ ) is weakly dependent on  $P_c$ . Variation factors are low (between 0.85 and 1.15) except for the O/F = 5.5 case, which is up to 1.45 between 80% and 100% power level.

One exception is R207 in figure 8. It decreases in value between 67% and 80% PL at O/F = 5.5 during test 29. This may indicate a hotter localized engine base heating condition at 67% PL than 80% PL. The hotter region may be caused by the two flow sheets coming off the ramps intersecting closer to the base of the engine at lower PLs. This agrees with Rocketdyne's localized engine base environments which are predicted to be maximum at low PL and O/F. Interestingly, during test 31, R207 increases rather than decreases with PL at O/F = 5.4. But it does show the least increase of all the wide angle instruments in this case. An explanation may be that the R207 FOV does not completely consist of the engine base region and the localized effect may be dominated in that case by other plume regions. This assertion is supported by the narrow view radiometer data discussed below.

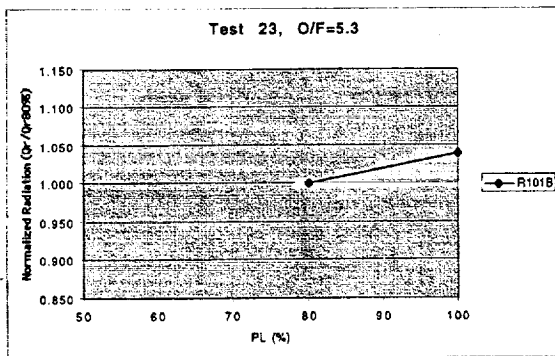


Figure 6, PL Trend at O/F = 5.3

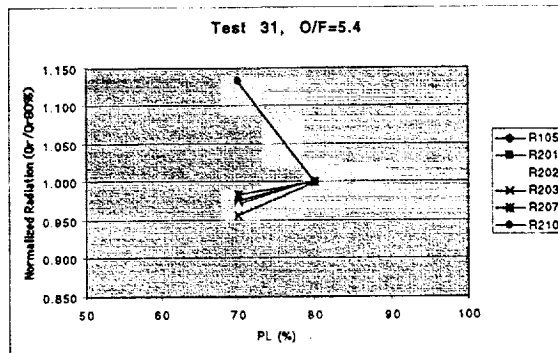


Figure 7, PL Trend at O/F = 5.4

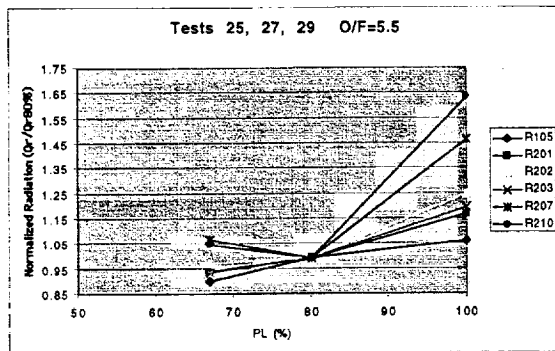


Figure 8, PL Trend at O/F = 5.5

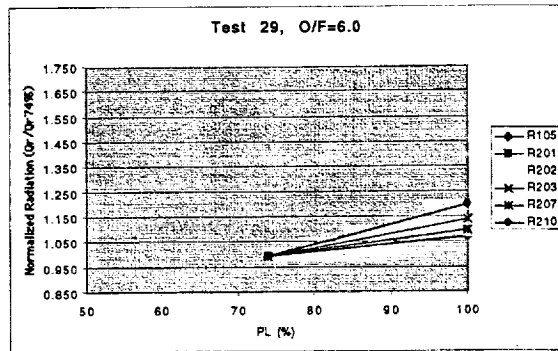


Figure 9, PL Trend at O/F = 6.0

Figures 10 and 11 show trends with varying O/F at constant PL. Data is normalized by O/F = 4.5 values for 57% power level and O/F = 5.5 values for 100% PL. Wide angle radiometer data generally increases with O/F. This makes intuitive sense since  $T_c$  is directly dependent on O/F. Variation factors are low (between 0.85 and 1.1) for both cases.

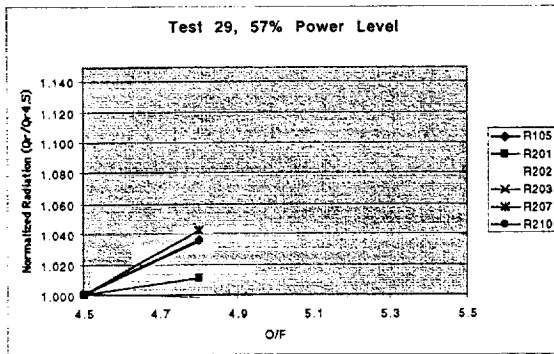


Figure 10, O/F Trend at 57% PL

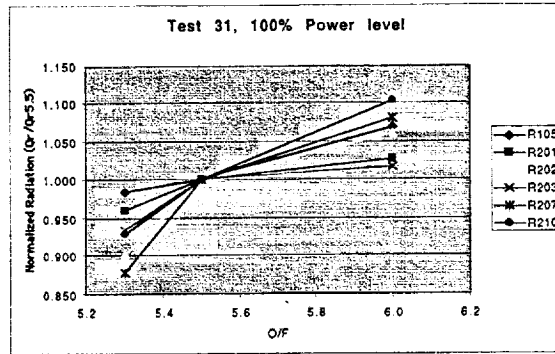


Figure 11, O/F Trend at 100% PL

All narrow view data are attenuated to some degree by EECO cooling water. So while their actual magnitudes may not be meaningful, trends from R210 may be useful in that they are different than wide angle trends in some cases. At a given PL, measured levels increase with O/F as do the wide angle instruments. But at both O/F conditions where power level increases from 67% or 70% to 80% (figures 7 and 8), narrow view levels decrease with increasing power level. This trend is similar but even stronger than that seen in R207 data. Since the narrow view radiometer has a FOV that only sees the engine base region, the stronger trend makes sense if the cause of it is higher plume radiation in the localized engine base region.

The most obvious source of error in the data is the EECO cooling water. It is not possible to determine the quantitative effect of the IEECO cooling water directly from the data since it was present on all tests. It almost certainly did affect the radiometer readings. Figure 5 shows that the cooling water is clearly aspirated into the base region.

Although the test by test data is not presented here, one can examine the difference between results for tests 27 through 30 versus test 31 results to get an idea of the effect of FEEECO cooling water. The primary radiometers were located to the ramp side of the engine on tests 27-31 to minimize the effects of the IEECO and FEEECO cooling water. Test 31 did not have FEEECO cooling water, while the preceding tests did. No clear trend can be seen from these data except for the higher narrow view instrument (R210) levels on test 31. This leads us to two conclusions: 1) The wide angle instruments are not significantly affected by cooling water from both EECO's versus just from the IEECO, and 2) The narrow view instrument is significantly affected by FEEECO cooling water. This makes sense since the cooling water can be seen circulating in the base region which encompasses the entire narrow view radiometer FOV, whereas this region is only one of the regions in the wide angle radiometer FOV's and is slightly upstream of the hottest plume region.

FEEECO ablator radiation is also clearly evident in figure 5. The radiation appears qualitatively significant in the visible wavelengths shown by the picture. FEEECO ablator radiation may partially explain why the inward facing radiometers (R202, R207) are closer to or slightly under predicted levels. While the ablative surface is obviously hot and radiating, its size is relatively small compared to the overall FOV of the wide angle instruments. It is outside the narrow view instrument FOV. So while it is certainly affecting the data, the amount of error introduced should be relatively small.

Instrument accuracy is quoted by the manufacturer (Medtherm, Inc.) as 0.1% of full scale. Pre- and post-test wide angle radiometer calibration variation is within -3.6% to +5.7%, which is a relatively low variation. The narrow view radiometer exhibited some damage to its sapphire window prior to test 27. At recalibration, and its post-test sensitivity was 35% lower than pre-test.

Several other possible sources of error exist, none of which significantly affect the data. Among these are the effects of the test stand aspirator on local plume static pressure, plume deflector re-radiation, and instrument location variability. The aspirator slightly reduces the plume size by enhancing entrainment of the surrounding air as the plume passes through the aspirator opening. Re-radiation from

the plume deflector should not be a problem since the deflector is approximately 56' from the bottom of the engine, is actively cooled, and is partially blocked by the aspirator. Finally, instruments were all hard mounted in place either by welds or bolts. Test to test variability in instrument location was therefore very small and should not be a significant source of error.

## COMPARISON TO PREDICTIONS

Ground test radiation data have been compared to sea level flight predictions. Two FDNS solutions were generated at sea level ambient pressure,  $M = 0.0$ :  $P_c = 857$  psia,  $O/F = 5.85$ , and  $P_c = 683$  psia,  $O/F = 5.43$ . The FDNS code is a state of the art, fully reacting Navier-Stokes flow field prediction code. Further plume prediction methodology details may be found in references 2, 3, and 4. Radiation predictions were made using the GASRAD band model gaseous radiation code<sup>5</sup>.

Plume induced radiation predictions were only made at two PL and O/F combinations. The 100% PL,  $O/F = 5.85$  case is compared to data from 100% PL tests at the two nearest O/F ratios, 5.5 and 6.0. The 80% PL,  $O/F = 5.43$  case is compared to 80% PL tests with  $O/F = 5.5$ . These comparisons are depicted graphically in figures 12 and 13.

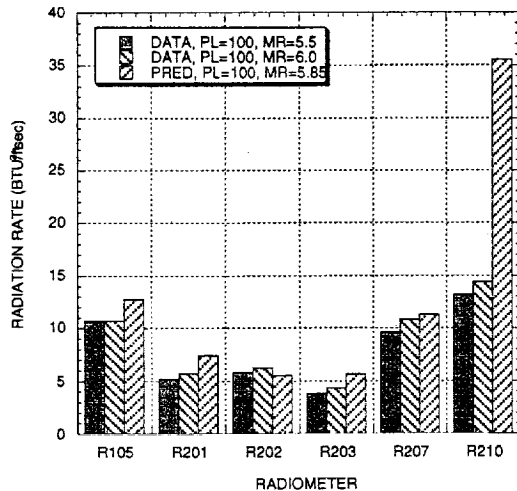


Figure 12, Data vs. Predictions, 100% PL

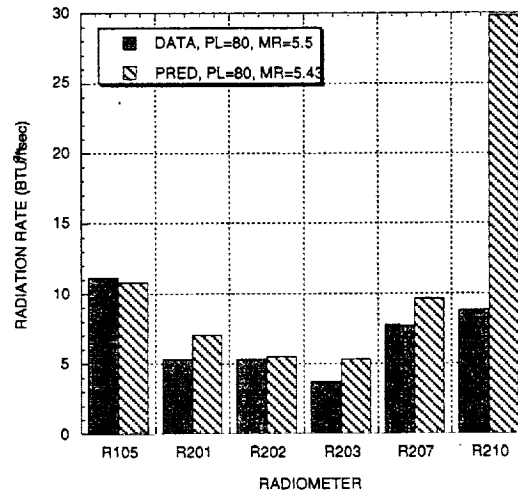


Figure 13, Data vs. Predictions, 80% PL

Predicted wide angle radiometer levels are within a range from 0.4 BTU/ft<sup>2</sup>\*sec below to 2.1 BTU/ft<sup>2</sup>\*sec above measured levels. This means the predicted levels were from 42% higher to 7% lower than the data.

In general, the wide angle radiometer predictions agree well with test data. Since the test data are generally overpredicted, flight environments generated using this predictive methodology should be slightly conservative, which is a desirable situation. Narrow view predictions are much higher than the data, which is to be expected since the narrow view data is significantly affected by EECO cooling water.

## SUMMARY

Plume radiation data was successfully collected for 9 tests of the X-33 XRS-2200 single linear aerospike engine at SSC Test Stand A-1. Tests prior to #27 had limited valid data due to cooling water effects. Several other possible sources of error were identified but were not found to be significant.

Measured data generally increased with increasing PL and O/F ratio. One exception was a decrease in local radiation levels in the engine base region with increasing PL. This agrees with Rocketdyne environment prediction trends for this region. Data agreed well with predictions. Predicted levels fell within a range from 7% below to 42% above measured data.

## REFERENCES

1. D'Agostino, Mark G., and Lee, Young C., "Test Data From X-33 XRS-2200 Linear Aerospike Single Engine Plume Radiation Measurements," TD63(00-0015), July 13, 2000.
2. Wang, Ten-See, "Analysis of Linear Aerospike Plume Induced X-33 Base-Heating Environment," Journal of Spacecraft and Rockets, Vol. 36, No. 6, November – December 1999, pp. 777-783.
3. Wang, Ten-See, ED32 (98-043), "Lockheed Martin Skunk Works (LMSW) X-33 CFD base thermal environment for Cycle 3.1 and Demonstrator Flight Instrument (DFI) trajectory points," November 24, 1998.
4. Wang, Ten-See, ED32 (98-045), "A comprehensive Lockheed martin Skunk Works (LMSW) X-33 three-dimensional CFD base thermal environment data reduction," December 1, 1998.
5. Reardon, John E., and Lee, Young C., "A Computer Program For Thermal Radiation From Gaseous Rocket Exhaust Plume (GASRAD)," Remtech Report RTR 014-9, December 1979.